Available online at www.sciencedirect.com
SCIENCE DIRECT
Journal of Power Sources 158 (2006) 485–496
JOURNAL OF POWER SOURCES
www.elsevier.com/locate/jpowsour

Steam reforming of methane over unsupported nickel catalysts

S. Rakass [a], H. Oudghiri-Hassani [a], P. Rowntree [a,1], N. Abatzoglou [b,*]

[a] *Département de chimie, Université de Sherbrooke, 2500 Boul. Université, Sherbrooke Quebec, Canada J1K 2R1*
[b] *Département de génie chimique, Université de Sherbrooke, Boul. Université, Sherbrooke, Quebec, Canada*

Received 30 June 2005; received in revised form 18 September 2005; accepted 19 September 2005
Available online 8 November 2005

Abstract

This paper describes a study of steam reforming of methane using unsupported nickel powder catalysts. The reaction yields were measured and the unsupported nickel powder surface was studied to explore its potential as a catalyst in internal or external reforming solid oxide fuel cells. The unsupported nickel catalyst used and presented in this paper is a pure micrometric nickel powder with an open filamentary structure, irregular 'fractal-like' surface and high external/internal surface ratio. CH_4 conversion increases and coke deposition decreases significantly with the decrease of CH_4:H_2O ratio. At a CH_4:H_2O ratio of 1:2 thermodynamic equilibrium is achieved, even with methane residence times of only ~0.5 s. The CH_4 conversion is $98 \pm 2\%$ at 700 °C and no coke is generated during steam reforming which compares favorably with supported Ni catalyst systems. This ratio was used in further investigations to measure the hydrogen production, the CH_4 conversion, the H_2 yield and the selectivity of the CO, and CO_2 formation. Methane-rich fuel ratios cause significant deviations of the experimental results from the theoretical model, which has been partially correlated to the adsorption of carbon on the surface according to TEM, XPS and elemental analysis. At the fuel: water ratio of 1:2, the unsupported Ni catalyst exhibited high catalytic activity and stability during the steam reforming of methane at low-medium temperature range.

Keywords: Steam reforming; Unsupported Ni catalyst; CH_4; Renewable fuels; GHG; Carbon deposition; XPS; SEM; TEM

1. Introduction

One of the most promising fuels for solid oxide fuel cell systems (SOFCs) is natural gas, which consists mainly of methane and is a naturally abundant resource. Hydrogen, which is one of the two major products of steam reforming of methane, is considered a clean energy source and its market demand is steadily increasing [1–3]. A viable fuel cell system requires (1) high-activity, (2) mechanical and chemical stability as well as (3) low production costs. Because nickel (Ni) is economical and highly active in steam reforming, ceramic-supported nickel catalysts are commonly used in steam reforming [4–21]. Although catalytically efficient, supported Ni catalysts suffer from deactivation by particle sintering and/or by reaction with supports, thermal deterioration (aging) of the support, and carbon deposition [4–10]. Rostrup-Nielsen et al. [4] have reported that the porous support can affect the sintering process and determine the final size distribution of the active surface Ni particles; the morphology of the support itself can also change under sintering conditions [4,6]. Phase transitions in the support and reactions between the support and active Ni particles can affect the sintering process, resulting in modification of the catalytic and mechanical properties of the composite material; although these changes may be reproducible, they are only poorly understood and rarely controllable.

Several approaches have been developed for minimizing the effects of carbon deposition during steam reforming of hydrocarbons. For example, the addition of potassium, magnesia, or molybdenum to supported Ni catalysts can stabilize the reforming catalysts by inhibiting the carbon formation or by promoting the carbon gasification [11–13]. However, it is clear that these types of composite catalysts are complex systems whose properties depend on the conditions of the successive stages of preparation and pretreatment. Thus, intensive research efforts are currently being carried out to improve both performance and lifetime of Ni-supported catalysts for steam reforming [14–19].

* Corresponding author. Tel.: +1 819 821 7904; fax: +1 819 821 7955.
E-mail addresses: Nicolas.Abatzoglou@USherbrooke.ca (N. Abatzoglou), Paul.Rowntree@USherbrooke.ca (P. Rowntree).
[1] Tel.: +1 819 821 7006; fax: +1 819 821 8017.

0378-7753/$ – see front matter © 2005 Elsevier B.V. All rights reserved.
doi:10.1016/j.jpowsour.2005.09.019

Roh et al. [14] have compared the catalytic activity of various supported Ni catalysts, Ni/α-Al_2O_3, Ni/SiO_2, Ni/ZrO_2, Ni/CeO_2, Ni/$MgAl_2O_4$, and Ni/Ce-ZrO_2, for methane steam reforming for CH_4:H_2O = 1:3 at 750 °C. These results show that Ni/Ce-ZrO_2 was highly active and remained stable by preventing carbon formation; however this system proved difficult to commercialize due to the high cost of the Ce-ZrO_2 support. Ni/SiO_2 catalysts had low catalytic activity or low hydrothermal stability (only 23% methane conversion). The deactivation of this catalyst resulted from the interaction between silica and Ni. Ni/CeO_2 exhibited only 55% methane conversion. Both Ni/ZrO_2 and Ni/$MgAl_2O_4$ showed high thermal stability and their CH_4 conversion were 77% and 79%, respectively. However, the Ni/$MgAl_2O_4$ catalyst did not show stability at the high space velocity of 288,000 h^{-1} cm^3 g^{-1}; its CH_4 conversion was initially 56% and decreased to 40% after only 3 h. Ni/α-Al_2O_3 catalysts showed an initial methane conversion of 72%, but the activity decreased gradually with time due to the formation of carbon. Thus, the CH_4 conversion dropped to 57% after only 200 min. Other studies [15,16] have shown that Ni/γ-Al_2O_3 was unstable at temperatures above 700 °C because of the thermal deterioration of the γ-Al_2O_3 support. This thermal deterioration causes sintering leading to pore closing and reduction in surface area as well as phase transition to α-Al_2O_3 at the active surface layer. Recently, Matsumura et al. [17] have studied the effects of supports such as silica, γ-alumina and zirconia in steam reforming of methane at 500 °C. They reported that the activity of nickel supported on silica, reduced with hydrogen at 500 °C, decreases due to the oxidation of nickel particles by steam during the reaction. Nickel supported on γ-alumina is difficult to reduce with hydrogen at 500 °C and is inactive in the reforming at 500 °C. Presently, Nickel supported on zirconia is among the most effective catalyst/support combinations for steam reforming at 500 °C [15,22]. These research works demonstrate that catalyst deactivation during steam reforming depends highly on the support. The carbon formation is largely dependent on the catalyst chemical composition as well as its preparation procedure as reported by many researchers [18,19]. It can be concluded that even though there are several developed Ni supported catalysts their use is still subject to significant constraints.

The present work presents a new approach to steam reforming, whereby these substrate-related complexities are avoided by considering unsupported nickel catalysts, with the ultimate goal being the development of simple and stable catalysts for in situ reforming processes of solid oxide fuel cells. The target temperature for our SOFC development project is ∼700 °C, due to the increasingly complex materials engineering problems that arise at higher temperatures. Preliminary results on the catalytic activity and behavior of different pure nickel powders in steam reforming of methane have been presented in a previous work [23]. We have shown that the morphology of the nickel powder plays a dominant role in determining the feasibility of the reforming process, and its temperature profile. An unsupported nickel catalyst with an open filamentary structure and irregular 'fractal' surface was found to be an efficient steam reforming catalyst; Ni powders with higher internal surface area were found to be less active, and have significantly higher onset temperatures for the steam reforming reaction. The outstanding issues associated with this approach are the long-term chemical and physical stability of the catalyst system, and the degree to which the reaction yields approach those associated with chemical equilibrium. In the present work, the catalytic activity and stability and carbon deposition have been investigated theoretically and experimentally for this unsupported 'fractal' Ni catalyst; our goal is to determine to what degree these systems are sensitive to the accumulation of carbonaceous deposits during reformer operation. We have found that for a CH_4:H_2O ratio of 1:2, the methane conversion was 98 ± 2% at 700 °C and no coke deposition was detected on the catalyst surface after 100 h of operation; the analysis of the product gases suggests that the system is very close to that calculated theoretically for thermodynamic equilibrium under the tested reaction conditions. The effects of varying the CH_4:H_2O ratio on the catalytic activity and coke deposition indicate experimentally that chemical equilibrium is not attained under methane-rich conditions. These initial measurements for fuel:water ratio of 1:2 are promising, and suggest that this new approach to catalyst development in SOFC applications may circumvent several of the traditional complexities of supported catalysts, while maintaining excellent levels of activity towards the steam reforming reactions.

2. Experimental methods

2.1. Catalyst characterization

The unsupported Ni catalyst used in this study (Inco Ni 255) is a pure nickel powder, with an open filamentary structure and irregular spiky surface; this powder is produced by the thermal decomposition of nickel tetracarbonyl [24]. The BET surface area (S_{BET} = 0.44 m^2 g^{-1}, particle size range of 1–20 μm) was measured at 77 K using a Quantachrome Autoasorb 1, assuming a 0.162 nm^2 cross-sectional area of N_2. The morphology of the catalyst was examined by scanning electron microscopy (SEM) using a JEOL JSM 840. Transmission electron microscopy (TEM) was carried out on a Hitachi H-7500 instrument working at 100 kV. Samples were dispersed in methanol and a drop of this dispersion was deposited on formvar-carbon coated nickel grid. The carbon content of the catalysts was determined using a Perkin-Elmer 240C Elemental Analyzer following removal from the reactor cell. X-ray photoelectron spectra (XPS) for catalyst samples were acquired at room temperature using a Kratos HS system with a monochromatized Al Kα ($h\nu$ = 1486.6 eV) X-ray source operated at 120 W; a 12000 μm^2 region of the sample was probed. The photoelectron kinetic energies were measured using a hemispherical electrostatic analyzer working in the constant pass energy mode. The background pressure in the analyzing chamber was kept below 2×10^{-8} Torr. Survey scans (0–1200 eV) and high-resolution Ni(3p), C(1s) and O(1s) spectra were obtained at pass energy of 160 and 40 eV, respectively. Correction for charging effects was achieved by referencing all binding energies with respect to the O(1s) core level spectrum in NiO (BE ≈ 529.1 eV [25]). The uncertainty in peak position is estimated to be ±0.2 eV for all spectra. The

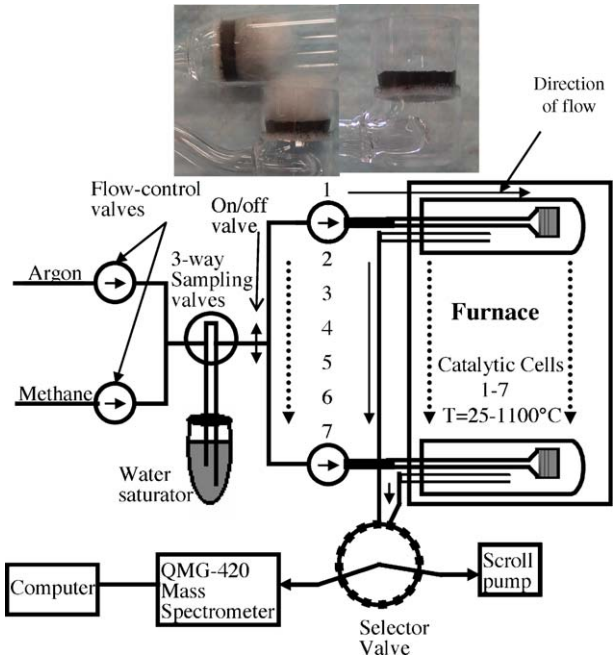

Fig. 1. Schematic view of the multicell reformer evaluation bench.

analysis of the measured Ni(3p), C(1s) and O(1s) high-resolution spectra envelopes was performed by curve-fitting synthetic peak components using the XPSPEAK41. The raw experimental data were used with no preliminary smoothing. Gaussian-Lorentzian product functions were used to approximate the line shapes of the fitting components. Shirley background subtraction procedures were used.

2.2. Catalytic activity characterization

Catalytic activity measurements were conducted at atmospheric pressure in a seven-cell differential reactor system that was constructed for real-time monitoring of the reforming reaction (Fig. 1). The experimental setup is equipped with a gas humidification system, a programmable furnace and a quadrupole mass spectrometer (Balzers QMG-420). The reactant gas is composed of CH_4 (Praxair, Ultra high purity), Ar (Praxair, Ultra high purity) and steam. The partial pressure of water in the gas is used to regulate the CH_4:H_2O ratio; it is fixed by controlling the temperature of the water through which the reaction gas was bubbled. The reaction gas was distributed equally among the 7 quartz reaction chambers such that different catalysts could be tested in the same time under identical conditions. The gas compositions and flow rates are controlled by rotameters (OMEGA). The flow rate used was 25 ml min^{-1} per tube. 0.25 g of catalyst is lightly packed into the inner quartz tubes and retained by quartz wool. The inner tubes include porous fused quartz disks (coarse porosity of 40–90 μm, 1.5 cm diameter), which supported the Ni catalyst beds (photo in Fig. 1). There is no entrainment of catalyst particles downstream because the catalyst pellet is already lightly compressed and during the early stages of the catalytic reaction there is sufficient sintering to preserve the integrity of the pellet. The mass-stability of the catalyst bed has been directly confirmed by gravimetry and the absence of any particles beyond the quartz wool following extended operation. The product gases from each reactor cell were sampled in a round-robin sequence using a computer-controlled valve assembly (Valco) and directed to the mass spectrometer for identification. The intensities of these measurements were calibrated using pure standard gases diluted in the Ar carrier gas. The accuracy is within ±3% and the reproducibility is ±2%. Temperature ramps were performed at a constant rate of 3 °C min^{-1} for all measurements. The temperatures reported herein were measured in the free-volume of the furnace system with a Type K thermocouple not used in the temperature control system. The measurement of the temperature at the surface of the catalyst was tested to determine if the endothermic nature of the reforming reaction caused significant cooling of the active surface. A thermocouple is placed on the surface of the Ni catalyst and another on the surface of the porous fused quartz disk. The temperatures at both places measured during these tests were equal and higher by 12 ± 2 °C than those measured in the free-space of the oven when the temperature in the latter is kept at 700 °C. Since the reaction is endothermic and there are additional heat transfer resistances for the gas flowing inside the reaction tubes this result seems contrary to the expectations. The difference observed is due to local temperature differences inside the oven due to uneven radiation emissivities and non-homogeneous convective current profiles.

In this study, CH_4 conversion, H_2, CO and CO_2 yields, the CO and CO_2 selectivities, and the gas hourly space velocity (GHSV) are defined as follows:

$$\mathrm{CH_4\ conversion}(\%) = \left(\frac{(P_{\mathrm{in\,CH_4}} - P_{\mathrm{out\,CH_4}})}{P_{\mathrm{in\,CH_4}}}\right) \times 100\%,$$

$$\mathrm{H_2\ yield}\,(\%) = \left(\frac{P_{\mathrm{H_2}}}{(P_{\mathrm{in\,CH_4}})}\right) \times 100\%,$$

$$\mathrm{CO\ selectivity}\,(\%) = \left(\frac{P_{\mathrm{CO}}}{(P_{\mathrm{CO}} + P_{\mathrm{CO_2}})}\right) \times 100\%,$$

$$\mathrm{CO_2\ selectivity}\,(\%) = \left(\frac{P_{\mathrm{CO_2}}}{(P_{\mathrm{CO}} + P_{\mathrm{CO_2}})}\right) \times 100\%,$$

$$\mathrm{CO\ yield}\,(\%) = \left(\frac{P_{\mathrm{CO}}}{(P_{\mathrm{CH_4\,in}})}\right) \times 100\%$$

$$\mathrm{CO_2\ yield}\,(\%) = \left(\frac{P_{\mathrm{CO2}}}{(P_{\mathrm{CH_4\,in}})}\right) \times 100\%,$$

$$\mathrm{GHSV} = \frac{F}{V}\,(\mathrm{h^{-1}}).$$

F is the volume of reaction mixture introduced per unit of time; V is the volume of catalyst.

2.3. Reaction pathways

In the steam reforming process of CH_4, the products are CO_2, CO, H_2 and solid carbon [26]. Methane is dissociated on the surface of Ni-based catalyst to form molecular hydrogen (Eqs. (1), (2) and (3)) and carbon on the catalyst surface (Eq. (3); this carbon can lead to catalyst deactivation [5,27–29] if it is not removed by reaction with water to form additional molecular hydrogen, carbon monoxide and carbon dioxide (Eqs. (5) and (6)). Additional carbon deposition can arise via the CO disproportionation reaction (Eq. (4)). The standard Gibbs free energy changes for these reactions all show significant temperature variations, and as such the equilibrium product distributions are highly sensitive to the operating conditions of the reformer system.

	300 °C		500 °C		700 °C	
	ΔG kJ/mol	ΔH kJ/mol	ΔG kJ/mol	ΔH kJ/mol	ΔG kJ/mol	ΔH kJ/mol
(1) $CH_4 + 2H_2O \rightarrow CO_2 + 4H_2$	61.29	177.95	19.40	185.14	−24.15	190.38
(2) $CH_4 + H_2O \rightarrow CO + 3H_2$	79.04	217.10	29.98	222.25	−20.17	225.42
(3) $CH_4 \rightarrow C + 2H_2$	25.64	82.67	5.05	86.79	−16.45	89.56
(4) $CO \rightarrow ½CO_2 + ½C$	−35.57	−86.79	−17.76	−86.29	−0.13	−85.45
(5) $C + H_2O \rightarrow CO + H_2$	53.40	134.43	24.93	135.46	−3.72	135.86
(6) $C + 2H_2O \rightarrow CO_2 + 2H_2$	35.65	95.28	14.34	98.36	−7.70	100.82
(7) $CO + H_2O \rightarrow CO_2 + H_2$	−17.74	−39.15	−10.59	−37.11	−3.98	−35.04

3. Results and discussions

3.1. Thermodynamic simulation

The sustainability of the reformer is governed by the thermal stability of the reforming catalyst and the deactivation of the catalyst by coke formation. To study the performance of methane steam reforming, the theoretical thermodynamic equilibrium conditions in the reforming reactor were calculated by minimizing the Gibbs free energy [30] using Factsage software and an in-house software simulation program. The purpose of these simulations is to identify thermodynamically favorable operating conditions for the methane steam reforming reaction, in terms of high methane conversion, low reactor temperature and minimal solid carbon deposition. The degree to which the true reaction products correspond to the equilibrium model will depend on several factors, the most important being the space velocity of the fuel gas across the catalytic system and the possible de-activation of the catalyst surface by carbon deposits.

To analyze the theoretical thermodynamic equilibrium of the steam reforming of methane reactor, the general reforming reaction can be written in the following way:

$$\alpha CH_4 + \beta H_2O \rightarrow \text{products}$$

In the simulation, the possible products are gaseous CH_4, H_2O, H_2, CO, CO_2 and solid C(s), which is presumed to have the thermodynamic properties of graphite. The stoechiometric coefficients, α and β correspond to a range of CH_4:H_2O ratios from 0.5–2.0. The temperature of the steam-reforming reactor is varied from 100–700 °C. Fig. 2 shows the calculated methane conversion, hydrogen yield, carbon deposition and the CO selectivity as a function of the CH_4:H_2O ratio (1:2 (10, 20 Torr), 1:1 (20, 20 Torr), 3:2 (30, 20 Torr) and 2:1 (40, 20 Torr)) and reaction temperature under a reaction pressure of 1 atm. As expected, the reforming yield of methane is strongly dependent on both temperature and the feed gas composition. The theoretical CH_4 conversion increases with increasing temperature for all CH_4:H_2O ratios investigated although complete conversion is possible only at low CH_4:H_2O ratios (Fig. 2a). Similar findings were reported by Liu et al. [31]. For a CH_4:H_2O ratio of 1:2, the theoretical thermodynamic equilibrium CH_4 conversion is 99% at 700 °C. Fig. 2b shows that the C(s) formation is strongly affected by the CH_4:H_2O ratio and temperature, with higher CH_4:H_2O ratios and reaction temperatures between 200 and 700 °C leading to increased carbon deposits on the catalyst. The modeling shows that with at CH_4:H_2O ratio of 1:2 no graphitic carbon is generated for any temperature considered herein. At lower CH_4:H_2O ratios, the steam reforming of methane dominates the reforming system and the high excess steam enhances the carbon gasification which suppresses the carbon deposition on the nickel reforming catalyst and therefore decreases the catalyst deactivation; the thermal cost of this excess steam load makes this mode of operation less favorable. Thus, the thermodynamic simulations indicate that a CH_4:H_2O ratio of 1:2 and temperatures near 700 °C provide favorable operating conditions.

3.2. Catalytic performance

3.2.1. Steam reforming of methane using unsupported nickel catalyst for CH_4:H_2O = 1:2

The steam reforming of methane for a 1:2 (10, 20 Torr) CH_4/H_2O molar ratio was monitored for 100 h (Fig. 3) by following the partial pressures of H_2, CO, CO_2 and CH_4. The onset of hydrogen production is approximately 325 °C; H_2 production increases as temperature increases, and the maximum yield was obtained at 500 °C. From 500 to 700 °C, hydrogen production was stable during time. The onset of carbon monoxide and carbon dioxide production was also approximately 325 °C. As can be seen in Fig. 3, H_2, CO and CO_2 yields are stable as the temperature is stabilized at T = 700 °C. Fig. 4 shows that the methane conversion is greater than 95% over the entire 100 h experimental duration. The results presented in Fig. 5 were obtained in a test-cell without the Ni catalyst, showing that the pyrolysis of

methane is negligible under the experimental conditions used for the steam reforming of methane.

Fig. 6 compares the experimental and theoretical temperature-dependent yields and selectivities of the product gases. With minor deviations, the agreement of the experimental and theoretical results is very good. Considering first the desired product of the steam reformer, we note that the onset of hydrogen production (Fig. 6a) is observed at 325 °C,

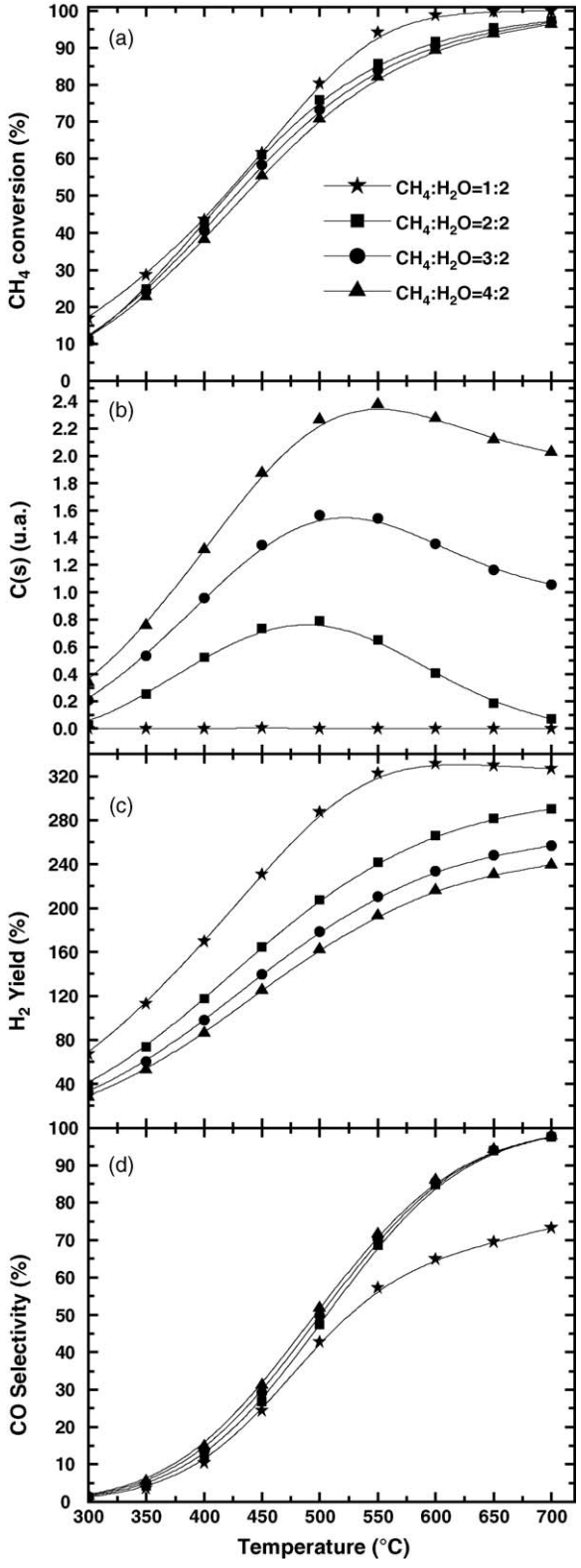

Fig. 2. Effects of temperature and CH_4:H_2O molar ratio, on theoretical equilibrium values of steam reforming reactor at 1 atm total pressure.

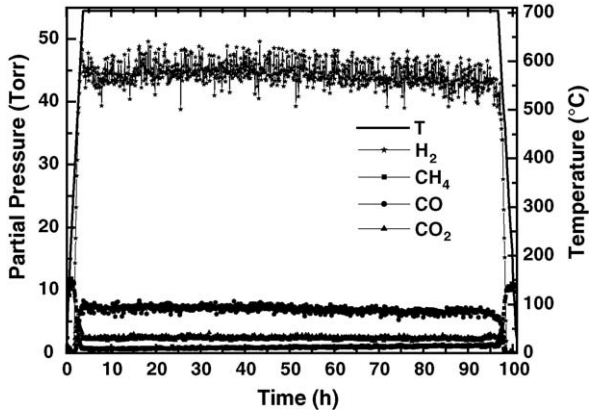

Fig. 3. Gas composition and temperature profiles vs. time on-stream for unsupporetd Ni catalyst. Reaction conditions: $P(CH_4) = 10$ Torr, $P(H_2O) = 20$ Torr, $P_{total} = 1$ atm, GHSV = 8500 h^{-1}.

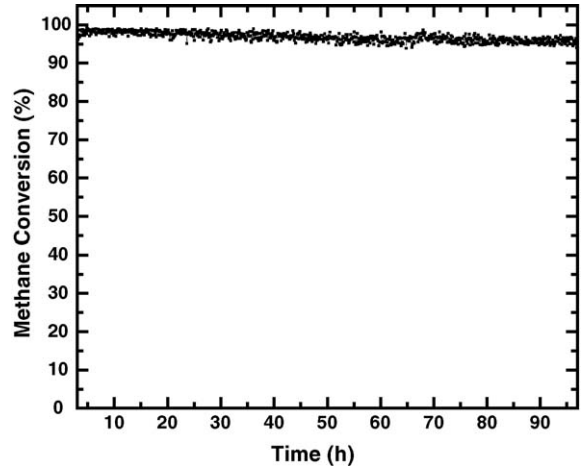

Fig. 4. Methane conversion stability over time for unsupported nickel catalyst. Reaction conditions: $T = 700$ °C for 95 h (time of reforming = 100 h), $P(CH_4) = 10$ Torr, $P(H_2O) = 20$ Torr, $P_{total} = 1$ atm, GHSV = 8500 h^{-1}.

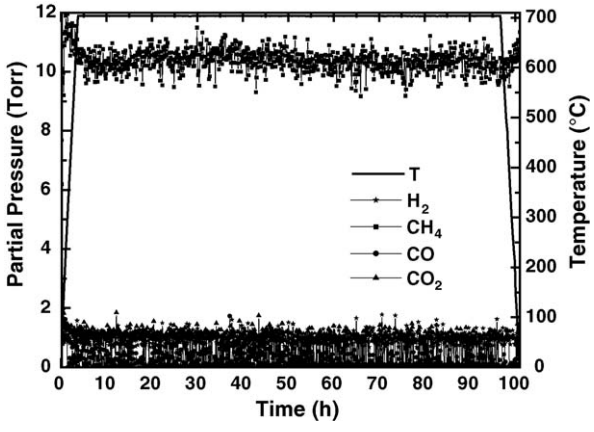

Fig. 5. Gas composition and temperature profiles vs. time on-stream for the blank. Reaction conditions: $P(CH_4) = 10$ Torr, $P(H_2O) = 20$ Torr, $P_{total} = 1$ atm, GHSV = 8500 h^{-1}.

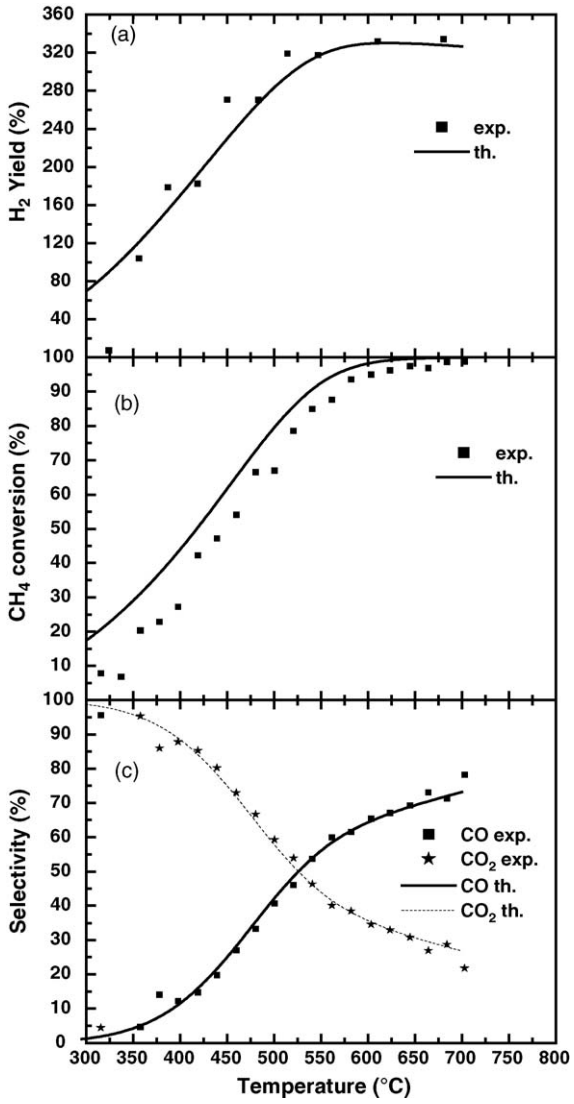

Fig. 6. (a) H_2 yield (%) (b) CH_4 conversion (%) and (c) CO selectivity (%), and CO_2 selectivity (%) over unsupported Ni catalyst during methane steam reforming. Symbols points, experimental values; solid line, theoretical equilibrium values. Feed gas composition: CH_4:H_2O = 10 Torr:20 Torr, P_{total} = 1 atm.

while the calculated onset is below 300 °C. This indicates that low-temperature activity is kinetically limited and that lower space velocities would be required to observe onset temperatures close to the theoretical predictions; since extremely low-temperature SOFC operation is not our objective, we have not pursued the study of this low-yield temperature regime. Methane conversion (Fig. 6b) is substantial for all temperatures above 400 °C, reaching 98 ± 2% at the ∼700 °C. We note that the experimental conversion tends to be 5–10% below the theoretical predictions in the intermediate temperature regime; the low-temperature onsets are also affected as described above for the H_2 yields. From 325 to 700 °C, thermodynamically and experimentally, the formation of increased quantities of CO and CO_2 is accompanied by a gradual increase in hydrogen formation. Expressed in terms of the associated selectivities, Fig. 6c shows that the experimental trends follow the theoretical equilibrium model. The longer-term stability of

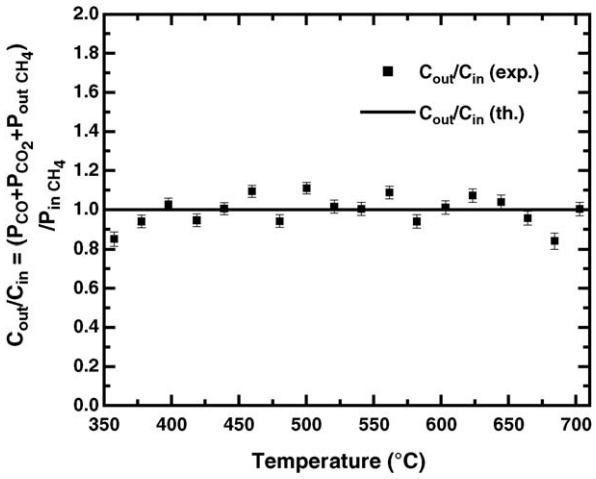

Fig. 7. Carbon balance obtained during methane steam reforming over unsupported Ni catalyst. Symbols points, experimental values; solid line, the expected value of 1 if there is no carbon deposition inside the reactor. Feed gas composition: CH_4:H_2O = 10 Torr:20 Torr, P_{total} = 1 atm.

the unsupported Ni reformer system was tested by continuous operation at 700 °C using the 1:2 fuel gas mixture. The methane conversion, hydrogen yield, and CO/CO_2 selectivities maintained their values shown in Fig. 6 for 100 h, indicating that there is no apparent decrease in catalyst activity on this time scale when using this fuel mixture.

Fig. 7 shows the experimental carbon balance (expressed as $(P_{CO} + P_{CO_2} + P_{out}CH_4)/P_{in\,CH_4}$) as a function of temperature for operation with the 1:2 fuel gas mixture. A value of 1 means that there is no solid carbon deposition at the surface of the catalyst. A value lower than 1 means that some carbon is missing at the reactor outlet and that there can be carbon deposition during the reaction. Since all points evaluated at different temperatures are randomly distributed around the value of 1, it can be concluded that there are not significant quantities of solid carbon deposited under these conditions. This result is also confirmed by the Elemental, the XPS and the TEM analyses that showed no detectable increases in carbon content following 9 h of operation, as well as the lack of catalyst deactivation during extended operation under these conditions. Table 1 provides the relative intensities of the total carbon with respect to the total nickel in fresh and used Ni catalysts. The decrease of the C(s) area coverage percentage from 58.5% to 11.5% after the use of the catalyst for 9 h shows that there is little or no deposition of carbon during the reforming reaction under these operating conditions with the feed gas mixture of CH_4:H_2O = 1:2. Fig. 8 shows a series of scanning electron microscopic images of the unsupported Ni

Table 1
Area ratio of carbon on nickel calculated in fresh Ni catalyst and used Ni catalyst during 9 h of steam reforming of methane (feed gas composition: CH_4/H_2O = 10 Torr:20 Torr, P_{total} = 1 atm), time of reforming = 9 h, T = 700 °C for 120 min)

Sample	Relative intensities (%) of C(1s)
Fresh Ni catalyst	58.5
Used Ni catalyst	11.5

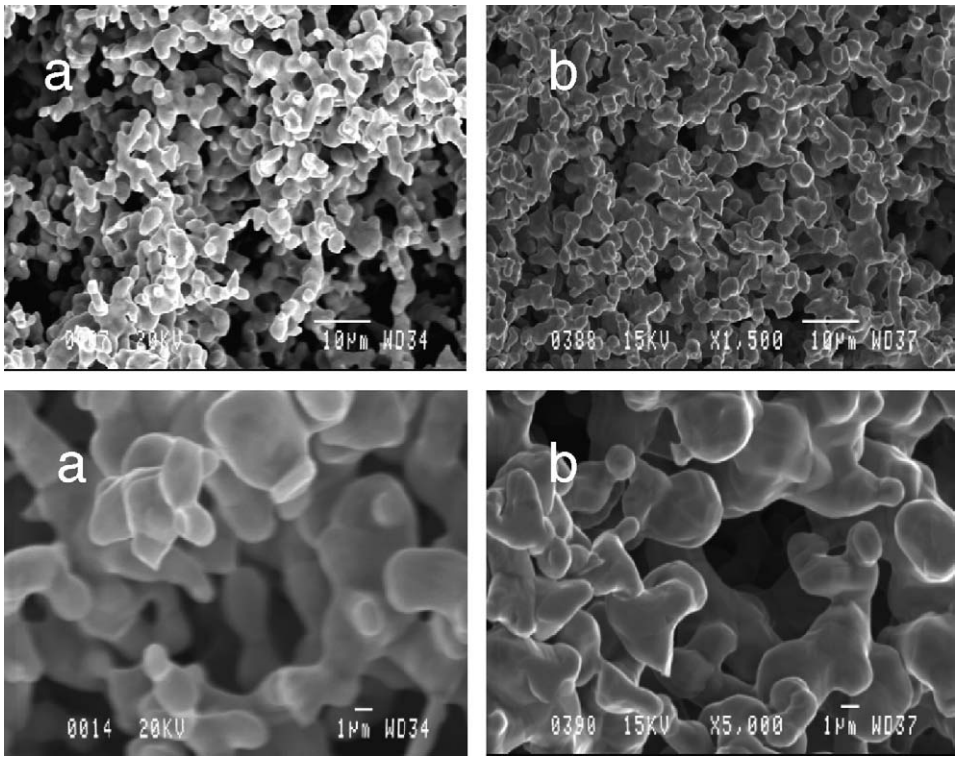

Fig. 8. Scanning electron micrographs of the Ni catalyst: (a) after a thermal treatment at temperature 700 °C and in Ar atmosphere (Time = 9 h, T = 700 °C for 120 min), (b) after CH_4 steam reforming during 9 h (reaction conditions: CH_4:H_2O = 1:2, P = 1 atm, time of reforming = 9 h, T = 700 °C for 120 min).

catalysts following simple heating to the operational temperature of 700 °C under a flowing Ar gas, and following 9 h of reforming activity using the 1:2 fuel gas mixture. Although the initial heating process does lead to some sintering, the catalysts do not suffer further morphological changes during the reforming operations, and there is no macroscopic accumulation of carbon particles that can be detected. The overall structure is extremely porous, as would be required for operation in a flow-through SOFC application.

3.2.2. Effects of sintering on catalytic activity

Sintering usually refers to the loss of active surface via a thermally activated structural transformation of the catalyst [4,6,8,10,19,21]. Sintering can significantly contribute to the deactivation of supported Ni catalyst [4,6,10,19,21] due to the reduction of the accessible catalytic surface and the blocking of pores. Two different but quite general models have been proposed for sintering of supported metal catalysts, i.e. the atomic migration and the crystallite migration models [19]. It has been reported that the presence of strong metal-support interactions affects the spreading, wetting and re-dispersion of the supported metals. Other factors can affect the stability of a metal crystallite towards sintering, e.g. shape and size of the crystallite, support roughness and pore size, impurities present in either the support or the metal [19,21].

Sintering occurs in both supported and unsupported metal catalysts. We have observed high catalytic activity (98 ± 2% at 700 °C for CH_4:H_2O ratio 1:2) and stability over the unsupported Ni catalyst used. Fig. 8 shows the SEM images of both used Ni catalyst after steam reforming of methane and the nickel catalyst subjected to a thermal treatment at temperature 700 °C under a pure Ar atmosphere. Fig. 8 shows that sintering does not appear to significantly reduce the available effective surface of catalyst in both cases. Remarkably, the quartz wool used to retain the nickel powders in the reactor tubes during the reformer evaluations appears to play an important role in maintaining the opening pores of the nickel catalyst, but the mechanism for this is not clear at this time; tests performed without the supporting quartz wool created highly distorted Ni samples, and considerable volume reduction due to sintering. Fig. 9 compares the pellet obtained after the steam reforming of methane using the quartz wool and that without the quartz wool, and shows the remarkable changes in the form of pellet. BET analysis of the quartz-supported nickel catalyst before and after thermal cycling shows that the specific surface does not decrease with the increase of temperature. We have previously reported that the catalytic activity of unsupported nickel catalyst in steam reforming of methane is dependent of the morphology of the nickel powders [23] and have suggested that the catalytic activity is approximately proportional to the external surface area of the catalyst as reported by Rostrup-Nielsen [4]. Thus, we can conclude that limited sintering of unsupported Ni catalyst during the steam reforming of methane has no significant effect on the catalytic activity via changes of the accessible surface area.

The results presented above demonstrate that reforming capabilities of the unsupported Ni catalysts conform closely to the theoretical predictions when operated with a CH_4:H_2O = 1:2 fuel gas ratio. The catalytic activity remains high over extended

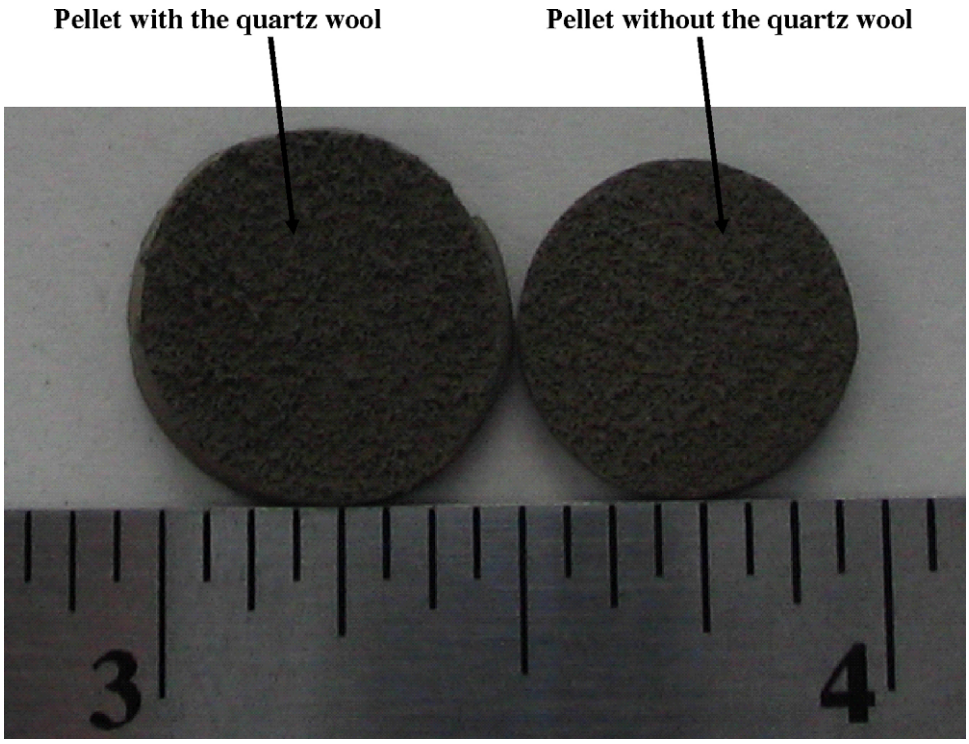

Fig. 9. Pellets obtained after the steam reforming of methane for 9 h using the quartz wool and that without the quartz wool. Reaction conditions: $P(CH_4) = 10$ Torr, $P(H_2O) = 20$ Torr, $P_{total} = 1$ atm, GHSV = 8500 h^{-1}.

periods of operation, and the sintering that takes place during operation at 700 °C does not impair the performance of the catalyst samples.

3.2.3. Variation of CH_4:H_2O ratio

In order to further compare the experimental and simulated systems, we have studied the effects of varying the CH_4:H_2O ratio on the catalytic activity of the nickel catalyst during methane steam reforming ($CH_4 + 2H_2O \rightarrow CO_2 + 4H_2$; $CH_4 + H_2O \rightarrow CO + 3H_2$). In agreement with the thermodynamic analysis described above (Fig. 2), the experimental methane conversion (Fig. 10) and hydrogen production (Fig. 11) are lowered by increasing the CH_4:H_2O ratio. At a CH_4:H_2O molar ratio of 1:1, the methane conversion (Fig. 10) increases with temperature and reaches its maximum (∼75%) at 590 °C, then decreases for higher temperatures (∼65 % of CH_4 conversion at $T = 700$ °C). The same behavior was observed when comparing two other methane-rich fuel ratios (3:2 and 2:1), where the maximum conversion of methane was found at ∼60%, followed by decreased conversion at higher temperatures. At 700 °C, only ∼40% and ∼30% of the available methane was converted for the two methane-rich fuel mixtures, respectively. This behavior is inconsistent with the simulation results, where for a given CH_4:H_2O molar ratio, higher temperatures systematically lead to higher theoretical equilibrium methane conversions; furthermore, the thermodynamic model indicates that the methane conversion is always in excess of 95% for these fuel gas mixtures. Once the target temperature of 700 °C is reached, the experimental methane conversions are stable over a period of 2 h for all gas mixtures studied, as shown in Fig. 12. This would suggest that

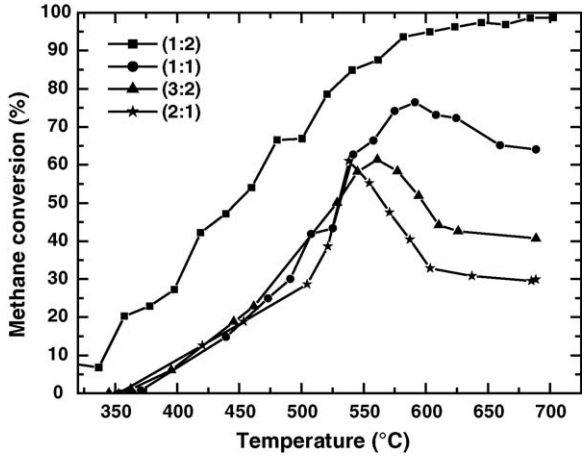

Fig. 10. Methane conversion over unsupported Ni catalyst as function of the CH_4:H_2O molar ratio and temperature. Reaction conditions: square symbol CH_4:H_2O = 1:2 (10 Torr:20 Torr); circle symbol CH_4:H_2O = 1:1 (20 Torr:20 Torr); up triangle symbol CH_4:H_2O = 3:2 (30 Torr:20 Torr) and star symbol CH_4:H_2O = 2:1 (40 Torr:20 Torr). For all studies the total gas pressure was 1.0 atm, with pure Ar carrier gas as the balance.

the reduced activity of the catalyst surfaces is associated with the thermal cycling of the catalysts in the 50–700 °C regime. We note that the theoretical equilibrium model predicts that these are the conditions that favor carbon deposition, as shown in Fig. 2. It is therefore possible that carbon deposition during this phase of the experiment contaminates the Ni catalysts and affects the performance even at higher temperatures where carbon deposition is not expected.

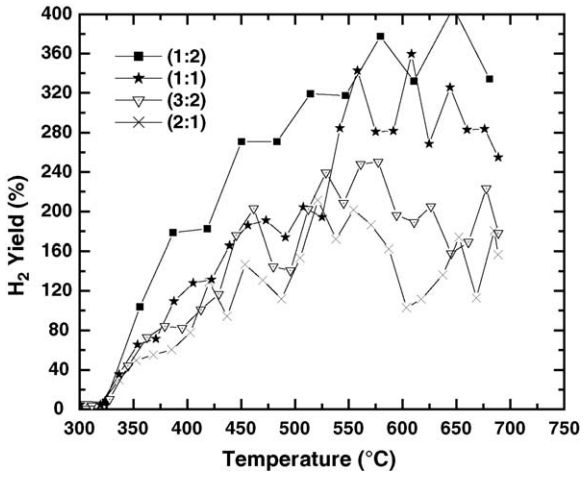

Fig. 11. Hydrogen yield over unsupported Ni catalysts as a function of the CH_4:H_2O molar ratio. Reaction conditions: square symbol CH_4:H_2O = 1:2 (10 Torr:20 Torr); star symbol CH_4:H_2O = 1:1 (20 Torr:20 Torr); down triangle symbol CH_4:H_2O = 3:2 (30 Torr:20 Torr) and cross symbol CH_4:H_2O = 2:1 (40 Torr:20 Torr). P = 1 atm, T = 700 °C, GHSV = 8500 h^{-1}.

In order to determine if carbon deposition is leading to partial catalyst deactivation, which in turn could lead to relatively lower expected methane conversions, elemental analysis for carbon content was performed on the unsupported catalysts following several hours of reformer operation using various fuel-steam mixtures. Table 2 shows that the carbon content following exposure to the 1:2 mixture is slightly less than that of the native Ni powder; for all catalysts exposed to the methane-rich mixtures the carbon content is significantly greater than that of the native powder, and the quantity of carbon increases with the CH_4:H_2O ratio. Thus, the reduced activity correlates well to the measured accumulation of carbon on the surface.

Further evidence of the conditions that lead to carbon deposition was obtained in a series of measurements whereby the unsupported Ni catalysts were heated to 700 °C under Ar and were used for steam reforming of methane for 2 h at 700 °C

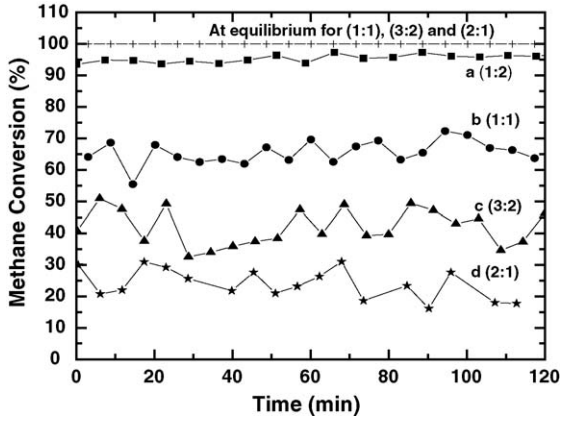

Fig. 12. Methane conversion over unsupported Ni catalysts as a function of the CH_4:H_2O molar ratio. Reaction conditions: square symbol CH_4:H_2O = 1:2 (10 Torr:20 Torr); circle symbol CH_4:H_2O = 1:1 (20 Torr:20 Torr); up triangle symbol CH_4:H_2O = 3:2 (30 Torr:20 Torr); star symbol CH_4:H_2O = 2:1 (40 Torr:20 Torr) and cross symbol for ratios (1:1), (3:2) and (2:1) at equilibrium. P = 1 atm, T = 700 °C, GHSV = 8500 h^{-1}.

Table 2
The effects of CH_4:H_2O molar ratio variation during steam reforming of methane on the average of carbon deposition on the unsupported nickel catalyst

CH_4:H_2O molar ratio	Carbon (%)[a]	Time of reforming (h)
1:2	0.04–0.03	9
1:1	0.88–0.88	9
3:2	1.37–1.41	17
2:1	1.89–1.86	9

[a] The Carbon (%) in fresh nickel catalyst is 0.16–0.21%. The uncertainty of measurement is 0.2%.

using the selected fuel gas mixtures then cooled to 50 °C under Ar. In the third series of measurements the samples were heated to 700 °C under Ar, then exposed to the fuel gas mixture of 3:2 for 2 h at 700 °C, and cooled to 50 °C. XPS analysis was performed for the three thermal profiles for three different fuel gas ratios to determine the conditions under which carbon deposition occurred, and to attempt the correlation with the observed catalytic activities.

Fig. 13(A)–(C) presents the XPS spectra of the C(1s) region for fuel gas mixtures of 1:1, 3:2 and 2:1, respectively. Within each panel, the topmost curve (Fig. 13(A)a, 13(B)c, and 13(C)f) corresponds to samples that were used for steam reforming of methane for 9 h (at temperatures from 50-700-50 °C with 2 h at 700 °C). The lowest curve corresponds to samples that were heated to 700 °C under Ar and were used for steam reforming of methane for 2 h at 700 °C then cooled to 50 °C under Ar (Fig. 13b, e and g); the middle curve of Fig. 13(B) shows the results of samples heated to 700 °C under Ar, then exposed to the fuel gas mixture of 3:2 for 2 h at 700 °C, and cooled to 50 °C (Fig. 13d). Three types of carbon can be identified in these spectra: amorphous 'coke' is detected at 283.7 eV binding energies as reported by Weckhuysen et al. [32] and Sexton et al. [33], graphitic carbon at 284.5 eV binding energies [34], and a peak associated with C=O is found at 288.6 eV binding energies. The graphitic components are present in similar quantities on catalysts used with the 1:2 fuel gas mixtures, and are even more evident on the unused catalyst surfaces; presumably the reduction of this peak during the reformer reaction is by direct oxidation. This is consistent with the elemental analysis results presented in Table 2. The C=O contribution (BE = 288.6 eV) also originates from the fresh Ni catalyst powder which is commercially produced by the thermal decomposition of $Ni(CO)_4$. Under prolonged operation the C=O contribution is also eliminated, as would be expected for operation under hydrogen rich (reducing) conditions. For each of the three fuel gas mixtures, we note the presence of extensive coke deposits for all samples that have been exposed to the methane-rich fuel mixtures at temperatures from 50-700-50 °C. This material can be created during heating or cooling cycles when exposed to the fuel gas at intermediate temperatures, as would be expected based on the theoretical thermodynamic modeling of the reaction process. It is also seen that samples that have been subject to operation at 700 °C (Fig. 13b, e and g) present only the types of carbon found on the native Ni powders, and as mentioned above, these components are reduced during the course of operation. The apparent lack of carbon deposition at 700 °C is somewhat surprising, insofar as

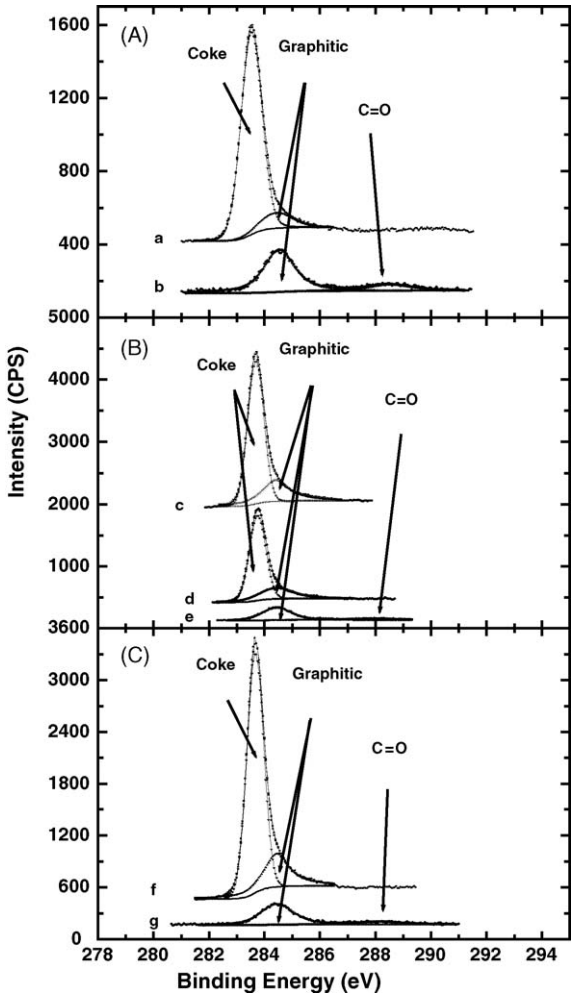

Fig. 13. XP C(1s) spectra for: Ni catalysts used for steam reforming of methane for 9 h for CH_4:H_2O ratios: (a) 1:1, (c) 3:2, (f) 2:1; Ni catalyst used for steam reforming of methane for 2 h at 700 °C after thermal treatment until 700 °C under argon carrier for CH_4:H_2O ratios (b) 1:1, (e) 3:2, (g) 2:1; Ni catalyst used for steam reforming of methane from 700 to 50 °C after thermal treatment until 700 °C under argon carrier gas for CH_4:H_2O ratio 3:2 (d).

the 3:2 and 2:1 mixtures should, in principal, deposit carbon even at 700 °C, as shown in Fig. 2. Thus, the XPS results confirm the accumulation of coke-like carbon on the surface at intermediate temperatures as predicted by theoretical thermodynamic modeling, while demonstrating that operation at 700 °C does not lead to carbon accumulation even under methane-rich conditions.

The above mentioned results would seem to support the hypothesis that the accumulation of carbon is linked to the reduced methane conversion shown in Figs. 10 and 12; indeed, this is one of the most common deactivation mechanisms for conventional supported Ni catalysts used in steam reforming reactions. However, this is not the case, and as such presents a remarkable difference between the operational use of the unsupported and supported catalyst systems. Fig. 14 shows the methane conversions measured for the catalysts that were only exposed to the fuel gas mixtures 1:1, 3:2, and 2:1 at 700 °C; the preheating process was during Ar flux as described above in the context of the XPS results (Fig. 13b, e and g). These results show that the initial CH_4 conversions obtained at $T = 700$ °C

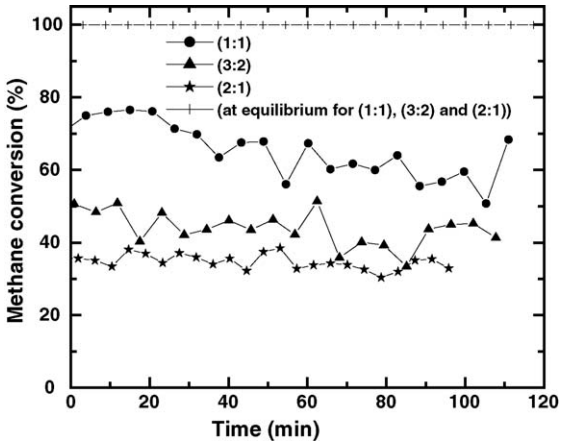

Fig. 14. Methane conversion obtained for the steam reforming of methane carried out for 2 h at 700 °C preceded by thermal treatment until 700 °C of the catalyst under argon carrier gas as a function of the CH_4:H_2O molar ratio. Reaction conditions: circle symbol CH_4:H_2O = 1:1 (20 Torr:20 Torr); up triangle symbol CH_4:H_2O = 3:2 (30 Torr:20 Torr); star symbol CH_4:H_2O = 2:1 (40 Torr:20 Torr) and cross symbol for ratios (1:1), (3:2) and (2:1) at equilibrium. $P = 1$ atm, $T = 700$ °C, GHSV = 8500 h^{-1}.

are ~75%, ~50% and ~35%, respectively; the conversions show systematic decreases over the 2 h reaction process, with the decrease being most pronounced with the 1:1 fuel mixture. By comparing these results (Fig. 14) with those obtained at $T = 700$ °C after steam reforming of methane for 9 h as described above when the catalysts were exposed to the fuel gas mixtures during the heating cycle (Fig. 12), we can conclude the following:

- For the 1:1 fuel mixture, the CH_4 conversions are similar to those obtained at $T = 700$ °C after steam reforming of methane for 9 h (Figs. 12 and 14);
- Similar results were obtained with the 3:2 fuel mixture (Figs. 12 and 14);
- For the 2:1 fuel mixture an increase of the CH_4 conversion from 25% (Fig. 12) to 35% (Fig. 14), related to the absence of carbon deposition, is observed.

For all methane-rich ratios, the methane conversions obtained experimentally are lower than those obtained theoretically (Figs. 12 and 14); the theoretical thermodynamic equilibrium is not reached. This is due to the fact that the space velocity in these experiments is higher than that of the basic experiment due to the increase of methane concentration in the gas flow. Thus, the decrease in methane conversion when the CH_4:H_2O molar ratio increases beyond 1:2 cannot be exclusively due to the carbon deposition on the catalyst surface, even in situations where the clear presence of this material on the catalyst surface was detected using both elemental and spectroscopic analysis.

Fig. 15 shows the simulated and the experimental CO/CO_2 ratios as function of the CH_4:H_2O ratios and reaction temperature under a reaction pressure of 1 atm. This figure confirms the previous conclusion that for CH_4:H_2O molar ratios 1:1, 3:2, and 2:1 the experimental equilibrium is not reached.

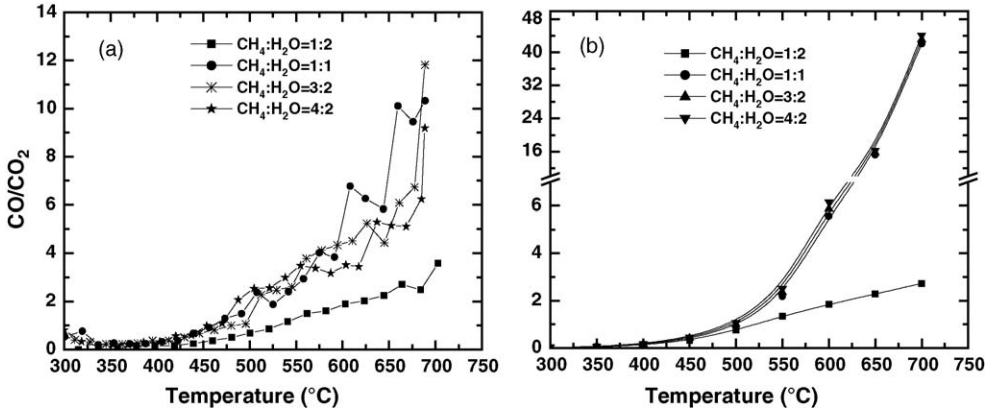

Fig. 15. The experimental (a) and the simulated (b) CO/CO_2 ratios obtained for the steam reforming of methane as function of the CH_4:H_2O ratios and reaction temperature under a reaction pressure of 1 atm.

For supported-Ni catalysts, many researchers have reported that both hydrogen produced and carbon deposition during steam reforming are strongly affected by the operating temperature and the methane/steam ratio [9,31,35]. When the CH_4:H_2O molar ratio is 1:2 methane conversion increased gradually as temperature increased to reach its maximum, $98 \pm 2\%$ at 700 °C. Fig. 4 indicates that the methane conversion was stable with time at 700 °C. These results compare well with the highest performances reported for supported-nickel catalysts. Dong et al. [20] have obtained 97% methane conversion over 15% Ni/Ce-ZrO_2 at 750 °C for CH_4:H_2O ratio of 1:3. Also, Roh et al. [15] have obtained 97% of methane conversion over Ni/Ce-ZrO_2/θ-Al_2O_3 catalyst for a CH_4:H_2O ratio of 1:3 at 700 °C. These present results demonstrate that the crucial role of the methane-to-steam ratio was also observed with the unsupported pure Ni powders. CH_4 conversion and hydrogen production increased significantly with decreasing CH_4:H_2O ratio.

4. Conclusion

These theoretical and experimental studies indicate that the CH_4 conversion increases and coke deposition decreases significantly with the decrease of CH_4:H_2O molar ratio during the steam reforming of methane over the unsupported Ni catalyst. For a CH_4:H_2O molar ratio of 1:2, the CH_4 conversion was $98 \pm 2\%$ at 700 °C. The onset of hydrogen production was approximately 325 °C. In addition, CH_4 conversion increased with increasing reaction temperature from 400 to 700 °C. The measured gas-phase concentrations of CH_4, H_2, CO, and CO_2 were in a good agreement with the theoretical equilibrium model using this fuel mixture; this indicates that the residence time of the feed gas over the metal surface was sufficient to reach equilibrium at the tested reaction conditions. The observed higher CH_4 conversion and H_2 yield suggest that the catalyst is very active for the steam reforming at low-to-medium temperatures.

For CH_4:H_2O molar ratios 1:1, 3:2, and 2:1, the methane conversions obtained experimentally are lower than those obtained theoretically. The decrease in methane conversion cannot be exclusively due to the carbon deposition on the catalyst surface; kinetic factors that prevent the reaction from reaching equilibrium appear to be the underlying reason for the lower than expected conversion rates.

For feed gases with a CH_4:H_2O molar ratio of 1:2, elemental analysis, XPS analysis, and TEM analysis demonstrated that there was no significant deposition of carbon on the catalyst surface; this explains the high and stable over time methane conversion ($98 \pm 2\%$ at 700 °C). The unsupported Ni catalyst, with an initially open filamentary structure and irregular spiky surface, presented high coke resistance as well as high catalytic activity and stability. Therefore, these materials are promising candidates for use in low-to-medium temperature SOFCs.

Acknowledgements

The authors greatly appreciate the many stimulating discussions with Prof. Hugues Menard (Dept of Chemistry, Université de Sherbrooke) concerning the sintering properties of the Ni powders used in this study.

We gratefully acknowledge the financial support of this work by NSERC (Natural Sciences and Engineering Research Council) and CFI (Canadian Foundation for Innovation).

References

[1] F.A. Coutelieris, S. Douvartzides, P. Tsiakaras, J. Power Sources 123 (2003) 200.
[2] R. Peters, R. Dahl, U. Klüttgen, C. Palm, D. Stolten, J. Power Sources 106 (2002) 238.
[3] J. Meusinger, E. Riensche, U. Stimming, J. Power Sources 71 (1998) 315.
[4] J.R. Rostrup-Nielsen, J. Sehested, J.K. Norskov, Adv. Catal. 47 (2002) 65.
[5] H.S. Bengaard, J.K. Nørskov, J. Sehested, B.S. Clausen, L.P. Nielsen, A.M. Molenbroek, J.R. Rostrup-Nielsen, J. Catal. 209 (2002) 365.
[6] J. Sehested, A. Carlsson, T.V.W. Janssens, P.L. Hansen, A.K. Datye, J. Catal. 197 (2001) 200.
[7] J.R. Rostrup-Nielsen, Catal. Today 37 (1997) 225.
[8] J.R. Rostrup-Nielsen, in: J.R. Anderson, M. Boudart (Eds.), Catalysis, science and Technology, vol. 5, Sprimger, Berlin, 1984, p. 1.
[9] D.L. Trimm, Catal. Today 37 (1997) 233.
[10] A.C.S.C. Teixeira, R. Giudici, Chem. Eng. Sci 54 (1999) 3609.
[11] T. Borowiecki, G. Wojciech, D. Andrzej, Appl. Catal. A: Gen. 270 (2004) 27.

[12] T. Borowiecki, A. Goiebiowski, B. Stasinska, Appl. Catal. A: Gen. 153 (1997) 141.
[13] L. Kepinski, B. Stasinska, T. Borowiecki, Carbon 38 (2000) 1845.
[14] H.-S. Roh, K.-W. Jun, W.-S. Dong, J.-S. Chang, S.-E. Park, Y.-I. Joe, J. Mol. Catal. A: Chem. 181 (2002) 137.
[15] H.-S. Roh, K.-W. Jun, S.-E. Park, Appl. Catal. A: Gen. 251 (2003) 275.
[16] H.-S. Roh, W.-S. Dong, K.-W. Jun, S.-E. Park, Chem. Lett. 30 (2001) 88.
[17] Y. Matsumura, T. Nakamori, Appl. Catal. A: Gen. 258 (2004) 107.
[18] J.R. Rostrup-Nielsen, J. Catal. 33 (1974) 184.
[19] P. Forzatti, L. Lietti, Catal. Today 52 (1999) 165.
[20] W.-S. Dong, H.-S. Roh, K.-W. Jun, S.-E. Park, Y.-S. Oh, Appl. Catal. A: Gen. 226 (2002) 63.
[21] C.H. Bartholomew, Appl. Catal. A: Gen. 212 (2001) 17.
[22] J. Blanchard, N. Abatzoglou, K. De Oliveira-Vigier, F. Gitzhofer, D. Gravelle, Proceedings of Science in Thermal and Chemical Biomass Conversion, Victoria Conference Center and Fairmont Hotel, Victoria, Vancouver Island, BC, Canada, 30 August to 2 September 2004 (2005) in press.
[23] S. Rakass, P. Rowntree, N. Abatzoglou, Proceedings of Science in Thermal and Chemical Biomass Conversion, Victoria Conference Center and Fairmont Hotel, Victoria, Vancouver Island, BC, Canada, 30 August to 2 September 2004 (2005) in press.
[24] F.V. Lenel, Powder Metallurgy, Principles and Applications, MPIF, Princeton, N.J., 1980, pp. 40.
[25] K.S. Kim, R.E. Davis, J. Electron Spectrosc. Related Phenomena 1 (1973) 251.
[26] T.V. Choudhary, D.W. Goodman, J. Catal. 192 (2000) 316.
[27] T.V. Choudhary, D.W. Goodman, Catal. Lett. 59 (1999) 93.
[28] V.C.H. Kroll, H.M. Swaan, C. Mirodatos, J. Catal. 161 (1996) 409.
[29] J. Xu, G.F. Froment, AIChE J. 35 (1989) 88.
[30] Y.-S. Seo, A. Shirley, S.T. Kolaczkowski, J. Power Sources 108 (2002) 213.
[31] Z.-W. Liu, K.-W. Jun, H.-S. Roh, S.-E. Park, J. Power Sources 111 (2002) 283.
[32] B.M. Weckuysen, M.P. Rosynek, J.H. Lunsford, Catal. Lett. 52 (1998) 31.
[33] B.A. Sexton, A.E. Hughes, D.M. Bibby, J. Catal. 109 (1988) 126.
[34] F. Larachi, H. Oudghiri-Hassani, M.C. Iliuta, B.P.A. Grandjean, P.H. McBreen, Catal. Lett. 84 (2002) 183.
[35] Z. Chen, Y. Yan, S.S.E.H. Elnashaie, Chem. Eng. Sci. 59 (2004) 1965.